19th Australasian Fluid Mechanics Conference
Melbourne, Australia
8-11 December 2014

Nanostructure analysis of in-flame soot particles in an automotive-size diesel engine

Y. Zhang, R. Zhang and S. Kook

School of Mechanical and Manufacturing Engineering
The University of New South Wales, Sydney, NSW 2052, Australia

Abstract

This paper presents experimental methods for direct sampling of in-flame soot particles and post-processing of their high-resolution transmission electron microscope (HR-TEM) images for the analysis of nanoscale internal structures. Soot particles from common-rail diesel engines are so small that can easily penetrate deep into the human pulmonary system, causing serious health issues. To shed some light on toxic soot particles formed within a diesel flame, the thermophoretic sampling and nanostructure visualisation of soot particles were performed in an automotive-size, single-cylinder diesel engine. The soot particles were collected onto a lacey TEM grid and then imaged in a HR-TEM. These images were post-processed using a Matlab code for key nanostructure parameters such as fringe length, tortuosity, and separation. The results show that diesel soot primary particles have two distinct nanoscale internal structures including amorphous cores and concentrically-oriented carbon-layer shells. For the tested conditions of this study, the fringe length, tortuosity, and separation are measured at 0.955, 1.22, and 0.399 nm, respectively. This well-developed technique will be applied to various engine combustion conditions in our future studies.

Introduction

Over the past 20 years, emission regulations for diesel engines have required reduction of exhaust particles by a factor of 30 [1]. One of the most widely used technologies to meet these regulations has been the high pressure injection (e.g. over 200 MPa) coupled with small nozzle holes (e.g. below 100 μm) [2], which can dramatically increase the mixing rate and thus mitigate soot formation. As a result, not only much less amount of soot emissions but also smaller particle sizes have been achieved in modern diesel engines [3-5]. A critical and ironic issue is that these small particles exhibit a much higher toxic and inflammatory potential than particles from old diesel engines operating under large black-smoke conditions. Smaller particles may penetrate more deeply into the respiratory tract, where their large surface-to-volume ratio could allow for more biological interactions [6]. Moreover, those particles appear to be more reactive and have defective bulk and surface structure to increase the toxicity [7], which, if regulated, will pose a significant challenge for engine developers.

Soot nanostructure refers to the characteristics of the internal carbon lamella (*i.e.* carbon layer plane segments) [8]. Their fringes are widely used to quantify nanostructures for carbon lamella orientation, fringe length (planar dimension of carbon layer plane), tortuosity (curvature of carbon layer) and fringe separation (the spacing between two adjacent carbon layers) [9]. These fringe parameters are related to chemical reactivity of soot particles such that shorter fringe length, higher tortuosity and fringe separation lead to higher soot oxidation [10-11]. However, toxicology studies suggested that higher reactivity means higher chance for soot particles to carry toxic chemicals that would in fact make a negative impact [6-7]. These important parameters are measured by performing high-resolution transmission microscope (HR-TEM) imaging of sampled soot particles and subsequent post-processing of the HR-TEM images [11-12].

Nanostructure analysis of in-flame soot particles were successfully conducted in a constant-volume combustion vessel simulating diesel-engine-like ambient and injection conditions [13-14]. These studies using Fischer-Tropsch diesel fuel (no naphthalene) reported that the mean fringe length, tortuosity and separation in soot primary particles are 0.98, 1.23, and 0.42 nm, respectively, which is similar to the soot particles sampled from ethanol flames in open flame burners [12]. Recently, one study [15] conducted in-cylinder soot particles sampling for nanostructure analysis in a diesel engine. The particles were collected by extracting soot-laden bulk gases inside the engine cylinder using a fast-response valve and then exposing a TEM grid to the gases. The findings are interesting that mature soot particles exhibited discernible core-shell structures. The decreased tortuosity and fringe separation, and increased fringe length during diesel combustion suggested the decreased reactivity of soot particle at later combustion stages.

Our recent studies [16-18] further improved the soot particles sampling technique by placing a sampling probe (holding a TEM grid at the tip) on the flame trajectory. The grid is directly exposed to a diesel flame inside the cylinder of a working diesel engine and therefore sample high number of soot particles for statistically meaningful morphology analysis [16]. This newly developed sampling technique has been used for the comparison between the in-flame and wall-deposited soot particles [17] as well as for the study about the variations of soot particle morphology with changing fuel injection timing and pressure [18]. However, our direct sampling technique has not been applied for the soot nanostructure analysis. This study aims to fill this gap. In this study, a lacey grid was placed in the sampling probe for HR-TEM imaging and the image analysis was conducted for the derivation of fringe length, tortuosity, and separation of soot primary particles.

Experiments

Diesel Engine and Operating Conditions

The in-flame soot sampling was carried out in an automotive-size, single-cylinder common-rail diesel engine. Detailed specification of the engine and its operating conditions are listed in Table 1. The diesel engine has a displacement of 498 cc with bore and stroke of 83 mm and 92 mm, respectively. The original combustion chamber had a compression ratio of 17.7. As shown in figure 1, a portion of the piston bowl-rim was removed to place a soot sampling probe within the trajectory of a diesel flame while avoiding its clash with moving engine parts. This modification decreased the compression ratio to 15.5, which is still within the range of production diesel engines (e.g. Mazda Skyactive-D). To simulate stable and warmed-up engine conditions, heated water with temperature of 90˚C was flowed through the engine head and cylinder block. The engine was naturally aspirated with the intake air temperature being fixed at

30˚C. The engine speed was held constant at 1200 revolutions per minute (rpm) using an electric motor.

The used fuel was a conventional ultra-low sulphur diesel with cetane number of 51. The fuel injection system was comprised of a Bosch second-generation common-rail and 7-hole solenoid injector, which is controlled by a universal injection and timing controller (Zenobalti 5100). The injector nozzle has 134-µm nominal hole diameter and the included angle of 150°. For a single-jet approach, six holes were blocked using a laser-welding technique. This approach was to isolate a fuel jet from complex jet-jet interactions. The common-rail pressure was fixed at 70 MPa and the injection duration at 2.34 ms (actual). The fuel mass per injection per hole (9 mg) corresponds to upper-mid to high-load engine condition where soot emissions are the most problematic. The injection timing was fixed at -6 crank angle degrees after top dead centre for (℃A aTDC) throughout the experiments. To monitor engine combustion conditions during the soot sampling experiments, the in-cylinder pressure was measured using a piezo-electric pressure transducer (Kistler 6056A), which was also used to calculate the apparent heat release rate.

Soot Sampling

Figure 1 shows the schematics of the engine combustion chamber and soot sampling system. The reacting diesel jet penetrated into the bowl-rim cut-out region where a sampling probe was housed. A 300-mesh, 150-µm thick lacey TEM grid (Emgrid LC300-Cu-150) was exposed to a sooting diesel flame during the main combustion event. Prior to the engine start, a new grid was loaded in the sampling probe. The engine was motored for a couple of minutes without fuel injection until the combustion chamber became thermally stable. The engine was skip-fired (1 fuel injection in 10 cycles) to expel residual gases from the previous firing cycle and at the same time minimise the thermal loading on quartz windows. A total of 10 fuel injections were executed for a given TEM grid, which was optimised for high enough number of soot particles for statistical analysis while avoiding soot overloading issues. The engine was stopped after the firing cycles followed by additional motoring cycles for complete exhaustion of combustion products, and then the grid was removed from the sampling probe and stored carefully for HR-TEM analysis.

Displaced volume	498 cc (single cylinder)
Bore	83 mm
Stroke	92 mm
Compression ratio	17.7 (original) 15.5 (modified)
Swirl ratio	1.4
Coolant temperature	90˚C
Intake air temperature	30˚C
Engine speed	1200 rpm
Fuel	Ultra low sulphur diesel
Cetane number	51
Common-rail	Second-generation Bosch
Nozzle	Minisac, hydro-grounded, K 1.5/0.86
Number of holes	7 holes (original) 1 hole (modified)
Hole diameter	134 µm (nominal)
Included angle	150˚
Rail pressure	70 MPa
Injection duration (actual)	2.34 ms
Injected mass per injection	9 mg
Injection timing	-6˚CA aTDC

Table 1. Engine specification and operating conditions

HR-TEM Image Processing and Analysis

The sampled soot particles were imaged using a HR-TEM (Philips CM200) with a point resolution of 0.25 nm and an acceleration voltage of 200 kV. A CCD camera with pixel resolution of 2688 by 2672 was used to record the soot particle images. The magnification settings of HR-TEM images were varied from x120,000 to x470,000 for the image clarify required for nanostructure analysis. Figure 2 (left) shows a less magnification image of the sampled in-flame soot aggregate adhering on the "string-like" structure of lacey TEM grid with a proportion of soot primary particles being blocked by the grid. To obtain an HR-TEM image of soot nanostructures, the selected particle area should not be overlapped with lacey grid layers or other primary particles.

The post-processing of HR-TEM images was conducted using a Matlab-based code developed by the Aizawa group at Meiji University [13]. The code selects a region of clear graphene fringes in the HR-TEM images and then converts them into binary images. The skeletons of these fringes were obtained by eroding their peripheries to a single pixel. Figure 2 (bottom-right) shows an example of a selected region in one of the soot primary particles. From these processed images, the fringes were indexed and the pixel number of the fringe skeletons was counted for the calculation of fringe length. The tortuosity (*i.e.* undulation of the fringes) was obtained using a ratio of the fringe length to the straight-line distance between the endpoints. For the calculation of fringe separation, pairs of two adjacent fringes were manually selected. The data of fringe length, tortuosity, and fringe separation in the present study were obtained from 5368 fringe skeletons and 1832 fringe pairs in 10 selected soot primary particles.

Results and Discussions

In-cylinder Combustion Conditions

The ensemble-averaged in-cylinder pressure and apparent heat release rate (aHRR) traces corresponding to the engine cycles of the soot particles sampling are shown in figure 3. The aHRR was calculated using a simple energy balance assuming ideal gas and steady conditions. The aHRR curve shows negative values indicating endothermic reaction due to evaporative cooling between the start of injection (SOI at -6 ℃A aTDC) and 5 ℃A aTDC. This is also evident in the in-cylinder pressure trace showing lower fired pressure than the motored pressure. The

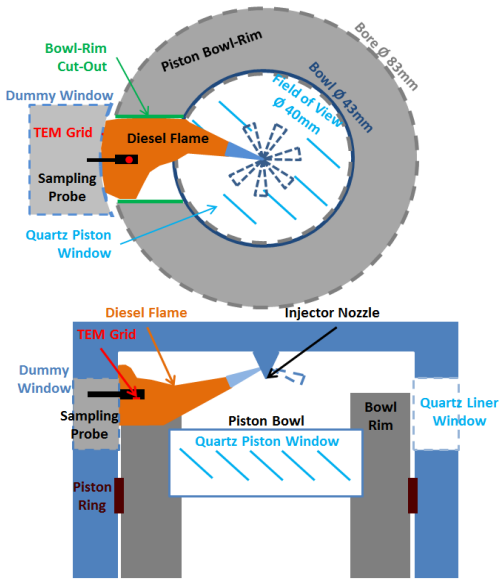

Figure 1. Illustration of the diesel engine and soot sampling system in the bottom-view (top) and side-view (bottom) orientations

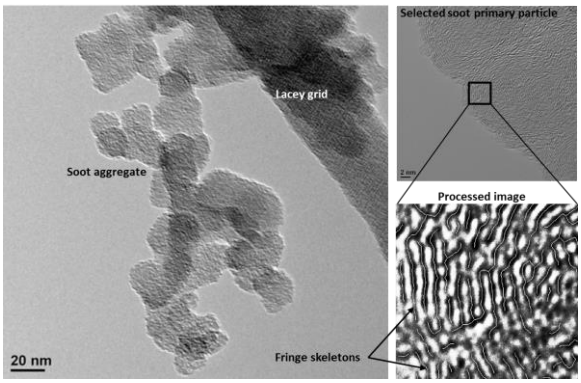

Figure 2. Soot aggregate image (left), selected primary particle (top-right) and processed image for fringe skeletons (bottom-right)

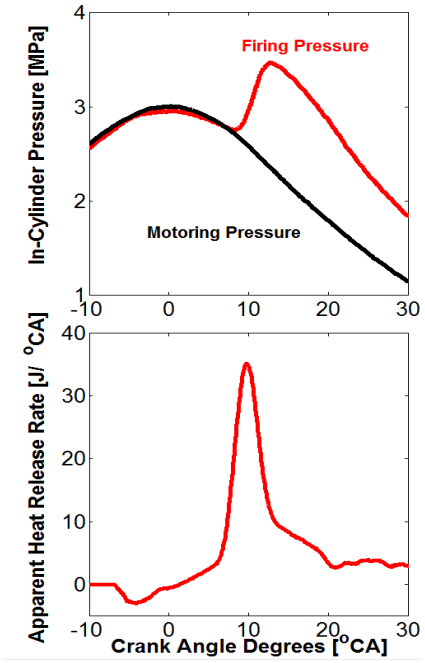

Figure 3. In-cylinder pressure and apparent heat release rate

fuel-air mixing occurred during this ignition delay period led to a rapid increase in the pressure and aHRR during the main combustion event.

HR-TEM Images

Figure 4 shows that the soot primary particles in a HR-TEM image appear as stacked graphene lamella comprised of the inner cores and outer shells (annotated by white dashed lines). This nanoscale structure is consistent with previous studies about diesel exhaust soot [19, 20]. From a visual inspection, it is clear that the inner core of soot primary particles present short graphene segments with random orientations. This amorphous inner core is concentrically surrounded by an outer shell comprised of extended graphitic carbon layers with apparent orientations. It was noted the reactivity would be higher in the core region than that in the outer region because the inner cores contain graphene segments that are much shorter than those formed in the outer shells. The shorter carbon layers with more edge-site carbon atoms typically mean higher reactivity [10-11].

Interestingly, one of the primary particles shown in figure 4 suggests two amorphous cores, which was explained that this multi-nucleation-site structure was created because the aggregates of small pre-formed particles formed the cores first, and then the surface growth occurred around the cores [20].

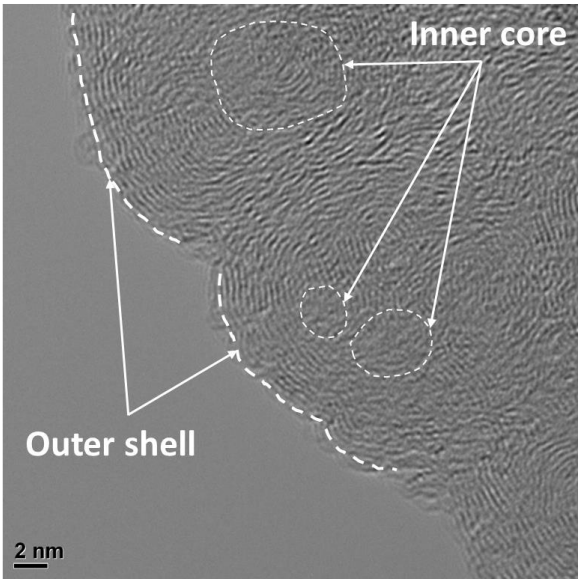

Figure 4. The nanostructure of inner core and outer shell soot primary particles

Nanostructure parameters

The fringe skeletons obtained from HR-TEM images can be used to calculate three key parameters for nanostructure characterisation of soot particles. These include fringe length, tortuosity, and separation. The fringe length is a measure of planar dimensions of carbon layer planes, indicating the plane size. As mentioned previously, the size of the carbon layer planes reflects the ratio of stable basal-plane and reactive edge-site atoms and therefore, longer fringe length means less reactivity [8, 15]. The tortuosity is a measure of fringe curvature, which rises from 5-membered or 7-membered rings within the carbon planes or from the bending and folding of a hexagonal sheet [8]. Therefore, higher tortuosity generally translates into higher reactivity. Similarly, higher fringe separation leads to higher reactivity.

In the present study, 10 primary particles similar to those in figure 4 were processed for more than 5000 fringe skeletons. This fringe data was used to obtain the size distributions of the fringe length, tortuosity, and fringe separation. Figure 5 shows the results. It is seen that most of the fringes are shorter than 3 nm and have tortuosity less than 2. The fringe separation is ranged between 0.3 and 0.6 nm. The mean values for the fringe length, tortuosity, and fringe separation are 0.955, 1.22 and 0.355 nm, respectively. Interestingly, these values are very close to those obtained from a constant-volume combustion vessel [13], suggesting similar reactivity between in-flame soot particles in the quiescent ambient gases and inside the engine cylinder. Future studies will be focused on the effect of engine operating conditions on these nanostructure parameters as well as a comparison of nanostructures between in-flame and exhaust soot particles.

Conclusion

The experimental method for the nanostructure analysis of soot particles sampled directly from a diesel flame inside the engine cylinder has been developed in the present study. Soot particles sampling and subsequent HR-TEM imaging was conducted in a single-cylinder, light-duty diesel engine employing a common-rail fuel injection system. The findings of this study are summarised as follows:

1. HR-TEM images reveal the nano-scale internal structures of soot primary particles. It is found that the in-flame soot

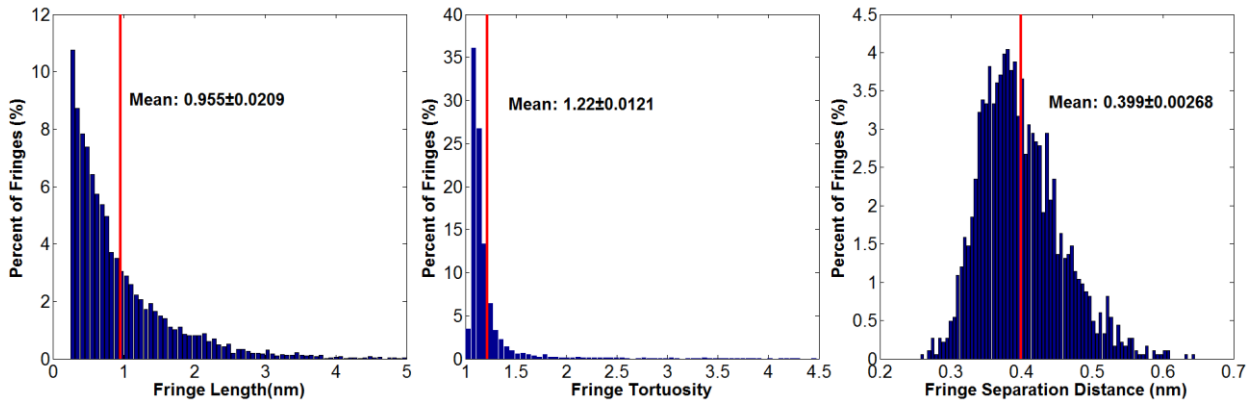

Figure 5. Histograms of fringe length (left), fringe tortuosity (middle), and fringe separation distance (right) for soot primary particles

particles consist of inner cores with amorphous carbon layer structures and outer shells with oriented graphitic carbon layers.

2. From 10 soot primary particles with 5368 fringe skeletons and 1832 fringe pairs, the mean values for the fringe length, tortuosity, and fringe separation are measured at 0.955, 1.22 and 0.399 nm, respectively. This result is consistent with the previous studies conducted in a constant-volume combustion vessel [13].

Acknowledgments

Experiments were conducted at the UNSW Engine Research Laboratory, Sydney, Australia. Support for this research was provided by the Australian Research Council via Discovery Project.

References

[1] U.S. Environmental Protection Agency, Health and Environmental Effects of Particular Matter. http://www.epa.gov/region7/air/quality/pmhealth.htm, 1997.

[2] Pickett, L. M. & Siebers, D. L. Non-Sooting , Low Flame Temperature Mixing-Controlled DI Diesel Combustion, *SAE Technical Paper*, **2004-01-1399,** 2004.

[3] Shi, J. P., Mark, D. & Harrison, R. M., Characterization of Particles from a Current Technology Heavy-Duty Diesel Engine. *Environ. Sci. Technol.*, **34,** 2000, 748–755.

[4] Park, K., Kittelson, D. B. & McMurry, P. H., Structural Properties of Diesel Exhaust Particles Measured by Transmission Electron Microscopy (TEM): Relationships to Particle Mass and Mobility. *Aerosol Sci. Technol.*, **38,** 2004, 881–889.

[5] Mathis, U., Mohr, M., Kaegi, R., Bertola, A. & Boulouchos, K., Influence of diesel engine combustion parameters on primary soot particle diameter. *Environ. Sci. Technol.*, **39,** 2005, 1887–92.

[6] Su, D. S. *et al.*, Cytotoxicity and inflammatory potential of soot particles of low-emission diesel engines. *Environ. Sci. Technol.*, **42,** 2008, 1761–1765.

[7] Frank, B. & Su, D. S., Diesel Soot Toxification. *Environ Sci Technol.*, **47,** 2013, 3026–3027.

[8] Vander Wal, R. L. & Mueller, C. J., Initial Investigation of Effects of Fuel Oxygenation on Nanostructure of Soot from a Direct-Injection Diesel Engine. *Energy & Fuels*, **20,** 2006, 2364–2369.

[9] Vander Wal, R. L., Tomasek, A. J., Pamphlet, M. I., Taylor, C. D. & Thompson, W. K., Analysis of HRTEM images for carbon nanostructure quantification. *J. Nanopart Res.*, **6,** 2005, 555–568.

[10] Vander Wal, R. L. Vander., Soot Nanostructure : Definition, Quantification and Implications Reprinted From : Diesel Exhaust Emission Control Modeling. *SAE Technical Paper*, 2005.

[11] Vander Wal, R. L. & Tomasek, A. J., Soot oxidation: dependence upon initial nanostructure. *Combust. Flame*, **134,** 2003, 1–9.

[12] Yehliu, K., Vander Wal, R. L. & Boehman, A. L., Development of an HRTEM image analysis method to quantify carbon nanostructure. *Combust. Flame*, **158,** 2011, 1837–1851.

[13] Sakai, M., Iguma, H., Kondo, K. & Aizawa, T., Nanostructure Analysis of Primary Soot Particles Directly Sampled in Diesel Spray Flame via HRTEM. *SAE Technical Paper*, **2012-01-1722,** 2012.

[14] Okabe, K., Sakai, M., Mizutani, Y. & Aizawa, T., Aromatic Additive Effect on Soot Formation and Oxidation in Fischer-Tropsch Diesel (FTD) Spray Flame -Morphology and Nanostructure Analysis of In-Flame Soot Particles via HRTEM. *SAE Int. J. Fuels Lubr.*, **6,** 2013, 807–816,

[15] Li, Z. *et al.*, Evolution of the nanostructure, fractal dimension and size of in-cylinder soot during diesel combustion process. *Combust. Flame.*, **158,** 2011, 1624–1630.

[16] Kook, S., Zhang, R., Szeto, K., Pickett, L. M. & Aizawa, T., In-Flame Soot Sampling and Particle Analysis in a Diesel Engine. *SAE Int. J. Fuels Lubr.*, **6,** 2013.

[17] Zhang, R., Szeto, K. & Kook, S., Size Distribution and Structure of Wall-Deposited Soot Particles in an Automotive-Size Diesel Engine. *SAE Int. J. Fuels Lubr.*, **6,** 2013.

[18] Zhang, R. & Kook, S., Influence of fuel injection timing and pressure on in-flame soot particles in an automotive-size diesel engine. *Environ. Sci. Technol.*, **48,** 2014, 8243–8250.

[19] Ishiguro, T., Takatori, Y. Akihama K., Microstructure of Diesel Soot Particles Probed by Electron Microscopy: First Observation of Inner Core and Outer Shell, *Combust. Flame*, **108,** 1991, 231-234.

[20] Lu, T., Cheung, C. S. & Huang, Z., Effects of engine operating conditions on the size and nanostructure of diesel particles. *J. Aerosol Sci.*, **47,** 2012, 27–38.